Inorganic Chemistry

ARTICLE

pubs.acs.org/IC

Electrochemical, Spectroscopic, and Photophysical Properties of Structurally Diverse Polyazine-Bridged Ru(II),Pt(II) and Os(II),Ru(II), Pt(II) Supramolecular Motifs

Jessica D. Knoll, Shamindri M. Arachchige, Guangbin Wang, Krishnan Rangan, Ran Miao, Samantha L. H. Higgins, Benjamin Okyere, Meihua Zhao, Paul Croasdale, Katherine Magruder, Brian Sinclair, Candace Wall, and Karen J. Brewer*

Department of Chemistry, Virginia Tech, 107 Davidson Hall, Blacksburg, Virginia 24061-0212, United States

ABSTRACT: Five new tetrametallic supramolecules of the motif $[\{(TL)_2M(dpp)\}_2Ru(BL)PtCl_2]^{6+}$ and three new trimetallic light absorbers $[\{(TL)_2M(dpp)\}_2Ru(BL)]^{6+}$ (TL = bpy = 2,2′-bipyridine or phen = 1,10-phenanthroline; M = Ru(II) or Os(II); BL = dpp = 2,3-bis(2-pyridyl)pyrazine, dpq = 2,3-bis(2-pyridyl)quinoxaline, or bpm = 2,2′-bipyrimidine) were synthesized and their redox, spectroscopic, and photophysical properties investigated. The tetrametallic complexes couple a Pt(II)-based reactive metal center to Ru and/or Os light absorbers through two different polyazine BL to provide structural diversity and interesting resultant properties. The redox potential of the $M^{II/III}$ couple is modulated by M variation, with the terminal $Ru^{II/III}$ occurring at 1.58−1.61 V and terminal $Os^{II/III}$ couples at 1.07−1.18 V versus Ag/AgCl. $[\{(TL)_2M(dpp)\}_2Ru(BL)](PF_6)_6$ display terminal M(dπ)-based highest occupied molecular orbitals (HOMOs) with the dpp(π^*)-based lowest unoccupied molecular orbital (LUMO) energy relatively unaffected by the nature of BL. The coupling of Pt to the BL results in orbital inversion with localization of the LUMO on the remote BL in the tetrametallic complexes, providing a lowest energy charge separated (CS) state with an oxidized terminal Ru or Os and spatially separated reduced BL. The complexes $[\{(TL)_2M(dpp)\}_2Ru(BL)]^{6+}$ and $[\{(TL)_2M(dpp)\}_2Ru(BL)PtCl_2]^{6+}$ efficiently absorb light throughout the UV and visible regions with intense metal-to-ligand charge transfer (MLCT) transitions in the visible at about 540 nm (M = Ru) and 560 nm (M = Os) ($\varepsilon \approx 33{,}000-42{,}000\ M^{-1}\ cm^{-1}$) and direct excitation to the spin-forbidden ^{3}MLCT excited state in the Os complexes about 720 nm. All the trimetallic and tetrametallic Ru-based supramolecular systems emit from the terminal Ru(dπ)→dpp(π^*) ^{3}MLCT state, $\lambda_{max}^{em} \approx 750$ nm. The tetrametallic systems display complex excited state dynamics with quenching of the ^{3}MLCT emission at room temperature to populate the lowest-lying ^{3}CS state population of the emissive ^{3}MLCT state.

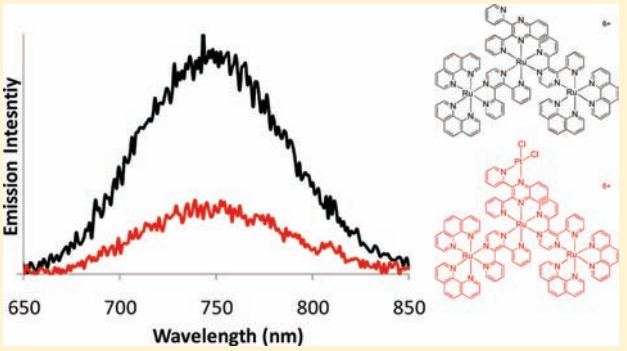

INTRODUCTION

Polyazine-bridged supramolecular complexes of Ru and Os have important applications in energy conversion and other light activated processes.[1−3] $[Ru(bpy)_3]^{2+}$ (bpy = 2,2′-bipyridine) is a well-known potent light absorber that can be optically excited into the ^{1}MLCT (metal-to-ligand charge transfer) excited state with UV or visible light to efficiently populate the emissive, long-lived ^{3}MLCT excited state. This ^{3}MLCT state can undergo excited state energy or electron transfer reactions useful in harnessing solar energy.[1−4] $[Os(bpy)_3]^{2+}$ expands the Ru analogue's light absorbing properties to longer wavelengths because of the ^{1}GS→^{3}MLCT absorption gaining intensity through spin−orbit coupling.[5−7] Component modification is widely used to tune the excited state properties of these complexes. Utilizing terminal ligands (TLs) such as phen (1,10-phenanthroline) and Ph_2phen (4,7-diphenyl-1,10-phenanthroline), Figure 1, tunes the light absorbing, redox, and excited state properties.[1,2,6,8] Replacing one or more TLs with a bridging ligand (BL) such as dpp (2,3-bis(2-pyridyl)pyrazine), dpq (2,3-bis(2-pyridyl)-quinoxaline), dpb (2,3-bis(2-pyridyl)benzoquinoxaline), or bpm (2,2′-bipyrimidine), Figure 1, allows the architecture to be expanded through incorporation of the light absorbers (LA) into supramolecular assemblies. Polyazine BLs provide motifs with considerable electronic coupling promoting electron or energy transfer.[3,9−12]

Covalently binding a reactive metal (RM) such as Pt^{II} to LAs has recently received increased interest applicable in solar energy conversion[13,14] and DNA modification.[15−20] Initial Ru,Pt bimetallic complexes reported were $[(bpy)_2Ru(bpm)PtCl_2]^{2+}$ (bpm = 2,2′-bipyrimidine)[21] as well as $[(bpy)_2Ru(dpp)PtMe_2]^{2+}$ and $[(bpy)_2Ru(dpp)PtCl_2]^{2+}$.[22] These complexes display Ru-based

Received: April 18, 2011
Published: August 23, 2011

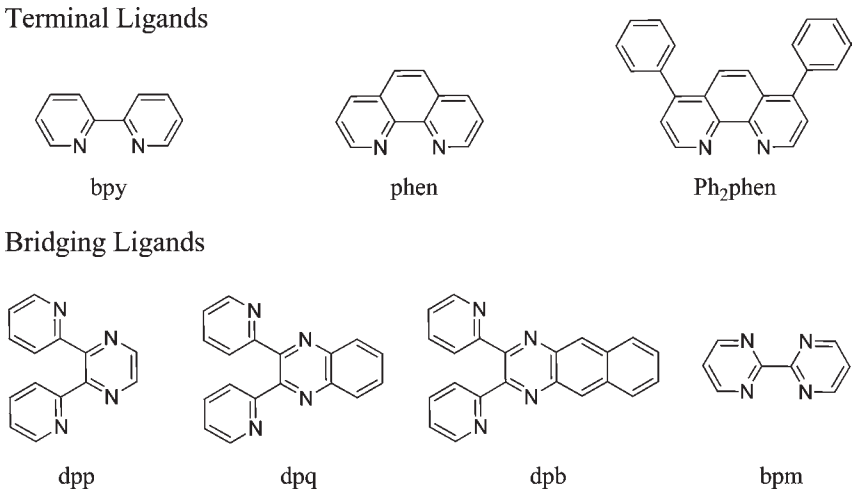

Figure 1. Polyazine terminal and bridging ligands. bpy = 2,2′-bipyridine, phen = 1,10-phenanthroline, Ph_2phen = 4,7-diphenyl-1,10-phenanthroline, dpp = 2,3-bis(2-pyridyl)pyrazine, dpq = 2,3-bis(2-pyridyl)quinoxaline, dpb = 2,3-bis(2-pyridyl)benzoquinoxaline, and bpm = 2,2′-bipyrimidine.

highest occupied molecular orbitals (HOMOs) and BL (dpp or bpm) based lowest unoccupied molecular orbitals (LUMOs). The nature of the substituent bound to Pt modulates the emission from the formally Ru(dπ)→dpp(π^*) ^{3}MLCT state, with $[(bpy)_2Ru(dpp)PtR_2]^{2+}$ and $[(bpy)_2Ru(bpm)PtR_2]^{2+}$ (R = Cl and CH_3, C_6H_5, $C_6H_4-CH_3$-*o*, $C_6H_4-OCH_3$-*p*, and C_6H_4-F-*p*).[23] The BL(π^*) reduction potential is shifted to less negative potential, and the emission energy from the Ru(dπ)→dpp(π^*) ^{3}CT state is red-shifted upon coordination of electron deficient Pt. The bimetallic complexes $[(bpy)_2M(BL)PtCl_2]^{2+}$, where M = Ru or Os and BL = dpq (2,3-bis(2-pyridyl)quinoxaline) or dpb (2,3-bis(2-pyridyl)-benzoquinoxaline), were reported to show similar BL(π^*) stabilization upon platination.[16] Complexes of the form $[(tpy)RuCl(BL)PtCl_2]^+$ (tpy = 2,2′:6′,2″-terpyridine; BL = dpp, dpq, or dpb),[18] $[(tpy)Ru(PEt_2Ph)(BL)PtCl_2]^{2+}$ (BL = dpp or bpm)[17] and $[(Ph_2phen)Ru(BL)PtCl_2]^{2+}$ (BL = dpp or dpq)[15] possess similar orbital energetics and are known DNA photobinding agents.

A series of Ru,Pt bimetallic complexes $[(bpy)_2Ru(phenNHCO(Rbpy))PtCl_2]^{2+}$ (R = COOH, COOEt, and CH_3) have recently been reported as photocatalysts in hydrogen production from water.[24,25] Electrochemical analysis shows that the LUMO is localized on the Rbpy moiety modified by variation of R. The complexes emit from the Ru(dπ)→phen(π^*) ^{3}CT excited state, and a nonemissive charge separated (CS) state was recently suggested to be competitively populated through intramolecular electron transfer to the Rbpy moiety. A dimer of this molecular architecture was formed by assembling two of the bimetallic complexes through the R positions with an ethylene diamine linker.[26] Multimetallic complexes such as $[Ru\{(dpq)PtCl_2\}_3]^{2+}$,[27] $[(bpy)_2Os(dpp)Ru\{(dpp)PtCl_2\}_2]^{4+}$,[28] and $[Os\{(dpp)Ru[(dpp)PtCl_2]_2\}_3]^{8+}$,[28] behave similarly with regard to BL(π^*) orbital stabilization upon coordination of the cis-$PtCl_2$ moiety. The two Os complexes display emission from only the Os(dπ)→dpp(π^*) ^{3}CT excited states.[28]

Reported herein are the synthesis and electrochemical, spectroscopic, and photophysical properties of five new structurally diverse $[\{(TL)_2M(dpp)\}_2Ru(BL)PtCl_2]^{6+}$ complexes (where TL = bpy or phen, M = Ru or Os, and BL = dpp, dpq, or bpm, Figure 2) and their trimetallic analogues $[\{(TL)_2M(dpp)\}_2Ru(BL)]^{6+}$. We reported $[\{(bpy)_2Ru(dpp)\}_2Ru(dpp)PtCl_2](PF_6)_6$[19] and $[\{(phen)_2Ru(dpp)\}_2Ru(dpq)PtCl_2](PF_6)_6$,[29] which displayed interesting properties prompting this analysis, and recently the tetrametallic complex $[\{(phen)_2Ru(dpp)\}_2Ru(dpq)PtCl_2](PF_6)_6$ was reported to reduce H_2O to H_2 with 115 turnovers in the presence of *N,N*-dimethylaniline electron donor when excited at 470 nm for 5 h.[29] This unique architecture combines two different types of Ru or Os LAs through two different polyazine bridging ligands and couples a RM center. Variation of M, BL, and TL provides a means of tuning orbital energetics and provides for the detailed analysis and considerable insight into the properties of this supramolecular architecture.

EXPERIMENTAL SECTION

Materials. $[(bpy)_2RuCl_2]$,[30] $[(phen)_2RuCl_2]$,[30] $[(bpy)_2OsCl_2]$,[31] $[(bpy)_2Ru(dpp)](PF_6)_2$,[9] $[(phen)_2Ru(dpp)](PF_6)_2$,[8] $[(bpy)_2Os(dpp)](PF_6)_2$,[32] $[\{(bpy)_2Ru(dpp)\}_2RuCl_2](PF_6)_4$,[33] $[\{(bpy)_2Os(dpp)\}_2RuCl_2](PF_6)_4$,[33] $[\{(phen)_2Ru(dpp)\}_2RuCl_2](PF_6)_4$,[29] $[\{(bpy)_2Os(dpp)\}_2Ru(dpq)](PF_6)_6$,[34] $[\{(bpy)_2Ru(dpp)\}_2Ru(dpq)](PF_6)_6$,[34] $[\{(bpy)_2Ru(dpp)\}_2Ru(dpp)](PF_6)_6$,[19] $[\{(phen)_2Ru(dpp)\}_2Ru(dpq)](PF_6)_6$,[29] $[\{(phen)_2Ru(dpp)\}_2Ru(dpq)PtCl_2](PF_6)_6$,[29] $[\{(bpy)_2Ru(dpp)\}_2Ru(dpp)PtCl_2](PF_6)_6$,[19] $[Pt(DMSO)Cl_2]$,[35] and dpq[36] were prepared as previously reported. The ligands bpy, phen, and dpp and $AgSO_3CF_3$ were purchased from Aldrich, and bpm and ethylene glycol were purchased for Alfa Aesar. $(NH_4)_2OsCl_6$, $RuCl_3\cdot 3H_2O$ and K_2PtCl_4 were purchased from Strem. Electrochemical grade Bu_4NPF_6 was purchased from Fluka. Spectral grade CH_3CN was purchased from Burdick and Jackson. Toluene, acetone, and methanol were purchased from Fisher ,and ethanol was purchased from Decon. All chemicals were used as received without further purification.

Synthesis of $[\{(bpy)_2Ru(dpp)\}_2Ru(bpm)](PF_6)_6$. The dichloro precursor, $[\{(bpy)_2Ru(dpp)\}_2RuCl_2](PF_6)_4$ (0.40 g, 0.20 mmol), was heated at reflux with $AgSO_3CF_3$ (0.25 g, 0.98 mmol) in 95% ethanol (20 mL) for 2 h. The AgCl precipitate was removed by filtration. The filtrate was brought back to reflux followed by addition of bpm (0.19 g, 1.2 mmol) dissolved in 95% ethanol (25 mL). The reaction mixture was heated at reflux for 24 h. Light was excluded at all times during the reaction. The reaction mixture was cooled to room temperature (RT). Aqueous NH_4PF_6 (1.0 g in 100 mL of water) was added to induce precipitation, and the product was collected by vacuum filtration. Purification was achieved on a Sephadex LH20 size exclusion column using 2:1 ethanol/acetonitrile as the mobile phase. The major (red) band which eluted first was collected by vacuum filtration. The product was dissolved in a minimal amount of acetonitrile (ca. 10 mL), syringe

dx.doi.org/10.1021/ic200793f |*Inorg. Chem.* 2011, 50, 8850–8860

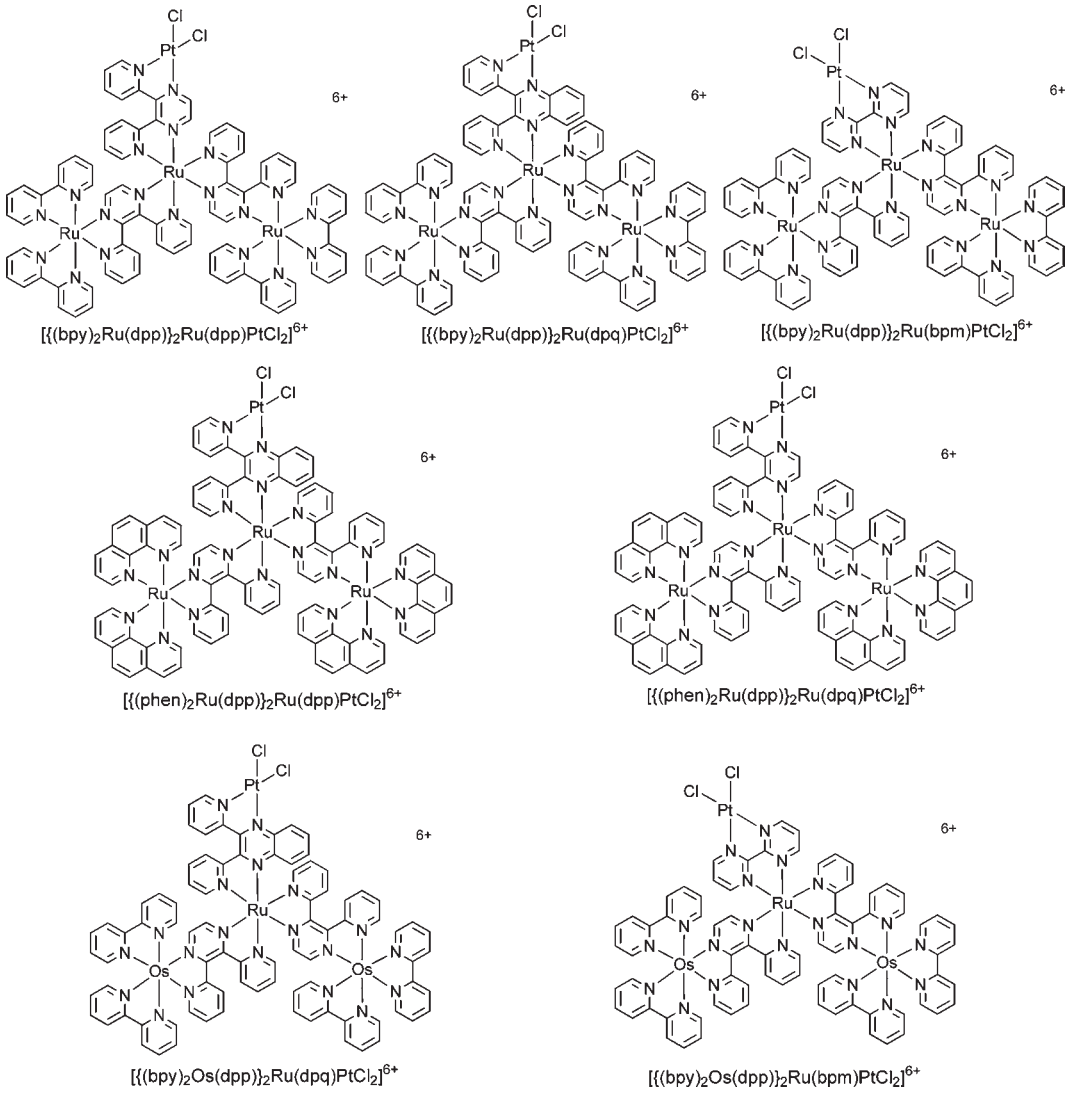

Figure 2. Molecular architectures for the $[\{(TL)_2M(dpp)\}_2Ru(BL)PtCl_2]^{6+}$ tetrametallic complexes, (bpy = 2,2′-bipyridine, phen = 1,10-phenanthroline, dpp = 2,3-bis(2-pyridyl)pyrazine, dpq = 2,3-bis(2-pyridyl)quinoxaline, bpm = 2,2′-bipyrimidine).

filtered and flash precipitated in diethyl ether (ca. 150 mL). The solid was collected by vacuum filtration, and dried under vacuum. Yield: 0.30 g, 0.13 mmol (63%). ESI-TOF MS: $[M - PF_6]^+$, m/z = 2280.

Synthesis of $[\{(phen)_2Ru(dpp)\}_2Ru(dpp)](PF_6)_6$. $[\{(phen)_2Ru(dpp)\}_2Ru(dpp)](PF_6)_6$ was prepared as above by substituting $[\{(phen)_2Ru(dpp)\}_2RuCl_2](PF_6)_4$ (0.35 g, 0.16 mmol) and dpp (0.30 g, 1.2 mmol). Yield: 0.28 g, 0.15 mmol (65%). ESI-TOF MS: $[M - 2PF_6]^{2+}$, m/z = 1153.

Synthesis of $[\{(bpy)_2Os(dpp)\}_2Ru(bpm)](PF_6)_6$. A mixture of $[\{(bpy)_2Os(dpp)\}_2RuCl_2](PF_6)_4$ (0.48 g, 0.22 mmol) and $AgSO_3CF_3$ (0.29 g, 0.11 mmol) were heated at reflux in 95% ethanol (20 mL) for 4 h. The AgCl precipitate was removed by filtration. The filtrate was added to bpm (0.21 g, 1.3 mmol) in 95% ethanol (20 mL) and heated at reflux for an additional 48 h. The reaction mixture was cooled to RT. Aqueous NH_4PF_6 (1 g in 50 mL of water) was added to induce precipitation, and the product was collected by vacuum filtration. Purification was achieved on a Sephadex LH-20 size exclusion column using 2:1 ethanol/acetonitrile as the mobile phase. The major (red) band was collected and solvent removed by vacuum. The product was dissolved in a minimal amount of acetonitrile (ca. 10 mL), syringe filtered, and flash precipitated in 200 mL of diethyl ether, collected by vacuum filtration, and dried under vacuum. Yield: 0.35 g, 0.13 mmol (60%). ESI-TOF MS: $[M - PF_6]^+$, m/z= 2458.2.

Synthesis of $[\{(bpy)_2Ru(dpp)\}_2Ru(bpm)PtCl_2](PF_6)_6$. A mixture of $[\{(bpy)_2Ru(dpp)\}_2Ru(bpm)](PF_6)_6$ (0.12 g, 0.046 mmol) and $[Pt(DMSO)_2Cl_2]$ (0.033 g, 0.071 mmol) were heated at reflux in 95% ethanol (30 mL) in the dark for 40 h. The reaction mixture was cooled to RT. Aqueous NH_4PF_6 (1.0 g in 50 mL of water) was added to induce precipitation, and the product was collected by vacuum filtration. The crude product was dissolved in a minimal amount of acetonitrile (ca. 10 mL), syringe filtered and precipitated in diethyl ether (50 mL). The product was collected by vacuum filtration and dried under vacuum. The product purity is controlled by stoichiometry and reaction conditions and is assayed via square wave voltammetry as all reactants and the product are redox active with distinctive redox couples. Yield: 0.085 g, 0.031 mmol (68%). ESI-TOF MS: $[M - PF_6]^+$, m/z = 2546.0.

Synthesis of $[\{(bpy)_2Os(dpp)\}_2Ru(bpm)PtCl_2](PF_6)_6$. $[\{(bpy)_2Os(dpp)\}_2Ru(bpm)PtCl_2](PF_6)_6$ was prepared as above by substituting $[\{(bpy)_2Os(dpp)\}_2Ru(bpm)](PF_6)_6$ (0.15 g, 0.057 mmol). Yield: 0.13 g, 0.045 mmol (79%). ESI-TOF MS: $[M - PF_6]^+$, m/z = 2724.1.

dx.doi.org/10.1021/ic200793f |*Inorg. Chem.* 2011, 50, 8850–8860

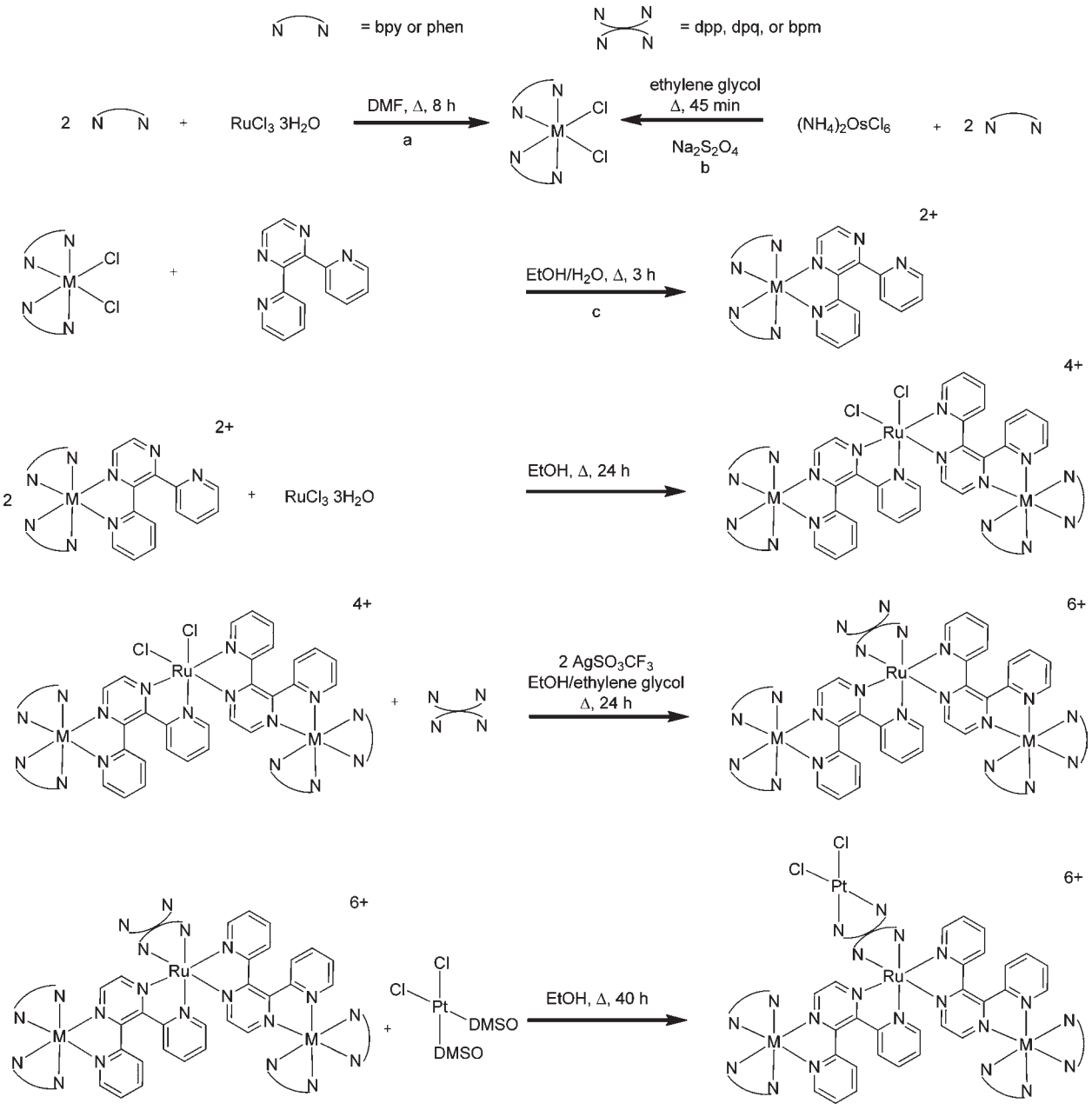

Figure 3. Building block process for the synthesis of the tetrametallic complexes. [a] From ref 30; [b] From ref 31; [c] From ref 9 (M = Ru, TL = bpy), 8 (M = Ru, TL = phen), and 32 (M = Os, TL = bpy).

Synthesis of [{(phen)$_2$Ru(dpp)}$_2$Ru(dpp)PtCl$_2$](PF$_6$)$_6$. [{(phen)$_2$Ru(dpp)}$_2$Ru(dpp)PtCl$_2$](PF$_6$)$_6$ was prepared as above by substituting [{(phen)$_2$Ru(dpp)}$_2$Ru(dpp)](PF$_6$)$_6$ (0.16 g, 0.060 mmol). Yield: 0.16 g, 0.056 mmol (94%). ESI-TOF MS: $[M - 2PF_6]^{2+}$, m/z = 1286.

Synthesis of [{(bpy)$_2$Ru(dpp)}$_2$Ru(dpq)PtCl$_2$](PF$_6$)$_6$. [{(bpy)$_2$Ru(dpp)}$_2$Ru(dpq)PtCl$_2$](PF$_6$)$_6$ was prepared as above by substituting [{(bpy)$_2$Ru(dpp)}$_2$Ru(dpq)](PF$_6$)$_6$ (0.15 g, 0.058 mmol). Yield: 0.16 g, 0.056 mmol (96%). ESI-TOF MS: $[M - PF_6 + H]^+$, m/z = 2673.

Synthesis of [{(bpy)$_2$Os(dpp)}$_2$Ru(dpq)PtCl$_2$](PF$_6$)$_6$. [{(bpy)$_2$Os(dpp)}$_2$Ru(dpq)PtCl$_2$](PF$_6$)$_6$ was prepared as above by substituting [{(bpy)$_2$Os(dpp)}$_2$Ru(dpq)](PF$_6$)$_6$ (0.10 g, 0.037 mmol). Yield: 0.066 g, 0.022 mmol (60%). ESI-TOF MS: $[M - PF_6 + 2H]^+$, m/z = 2852.

ESI-MS. Electrospray ionization (ESI) mass spectrometry was performed using an Agilent Technologies 6220 Accurate-Mass TOF LC−MS with a dual ESI source.

Electrochemistry. Cyclic voltammetry and Osteryoung square wave voltammetry were performed with an Epsilon potentiostat from Bioanalytical Systems, Inc. in a one compartment, three electrode cell using a carbon working electrode, platinum wire auxiliary electrode, and Ag/AgCl reference electrode calibrated against the ferrocene/ferrocenium couple, $FeCp_2/FeCp_2^+$, as an internal standard (0.46 V versus Ag/AgCl). Measurements were made at a rate of 100 mV/s. The supporting electrolyte was 0.1 M Bu_4NPF_6 in spectral grade acetonitrile. Solutions were deoxygenated by bubbling with argon, and the working electrode was manually cleaned prior to analysis.

Electronic Absorption Spectroscopy. Electronic absorption spectra were obtained with an Agilent 8453 UV−vis spectrophotometer

dx.doi.org/10.1021/ic200793f |Inorg. Chem. 2011, 50, 8850–8860

Table 1. Electrochemical Data for a Series of Complexes $[\{(TL)_2M(dpp)\}_2Ru(BL)]^{6+}$ and $[\{(TL)_2M(dpp)\}_2Ru(BL)PtCl_2]^{6+}$.[a]

complex	$E_{1/2}$ (V) versus Ag/AgCl			
	oxidation	reduction		
		Trimetallics		
$[\{(phen)_2\mathbf{Ru}(dpp)\}_2Ru(\mathbf{dpp})]^{6+}$	1.61 ($2\mathbf{Ru}^{II/III}$)	−0.45 ($dpp^{0/-}$)	−0.59 ($dpp^{0/-}$)	−1.00 ($\mathbf{dpp}^{0/-}$)
$[\{(phen)_2\mathbf{Ru}(dpp)\}_2Ru(\mathbf{dpq})]^{6+}$[b]	1.56 ($2\mathbf{Ru}^{II/III}$)	−0.42 ($dpp^{0/-}$)	−0.59 ($dpp^{0/-}$)	−0.80 ($\mathbf{dpq}^{0/-}$)
$[\{(bpy)_2\mathbf{Ru}(dpp)\}_2Ru(\mathbf{dpp})]^{6+}$[c]	1.58 ($2\mathbf{Ru}^{II/III}$)	−0.50 ($dpp^{0/-}$)	−0.64 ($dpp^{0/-}$)	−1.08 ($\mathbf{dpp}^{0/-}$)
$[\{(bpy)_2\mathbf{Ru}(dpp)\}_2Ru(\mathbf{dpq})]^{6+}$[d]	1.58 ($2\mathbf{Ru}^{II/III}$)	−0.42 ($dpp^{0/-}$)	−0.62 ($dpp^{0/-}$)	−0.82 ($\mathbf{dpq}^{0/-}$)
$[\{(bpy)_2\mathbf{Ru}(dpp)\}_2Ru(\mathbf{bpm})]^{6+}$	1.59($2\mathbf{Ru}^{II/III}$)	−0.56 ($dpp^{0/-}$)	−0.70 ($dpp^{0/-}$)	−1.08 ($\mathbf{bpm}^{0/-}$)
$[\{(bpy)_2\mathbf{Os}(dpp)\}_2Ru(\mathbf{bpm})]^{6+}$	1.16 ($2\mathbf{Os}^{II/III}$)	−0.56 ($dpp^{0/-}$)	−0.67 ($dpp^{0/-}$)	−1.06 ($\mathbf{bpm}^{0/-}$)
$[\{(bpy)_2\mathbf{Os}(dpp)\}_2Ru(\mathbf{dpq})]^{6+}$[d]	1.07 ($2\mathbf{Os}^{II/III}$)	−0.56 ($dpp^{0/-}$)	−0.71 ($dpp^{0/-}$)	−0.88 ($\mathbf{dpq}^{0/-}$)
		Tetrametallics		
$[\{(phen)_2\mathbf{Ru}(dpp)\}_2Ru(\mathbf{dpp})PtCl_2]^{6+}$	1.63 ($2\mathbf{Ru}^{II/III}$)	−0.32 ($\mathbf{dpp}^{0/-}$)	−0.51 ($dpp^{0/-}$)	−0.63 ($dpp^{0/-}$)
$[\{(phen)_2\mathbf{Ru}(dpp)\}_2Ru(\mathbf{dpq})PtCl_2]^{6+}$[b]	1.58 ($2\mathbf{Ru}^{II/III}$)	−0.05 ($\mathbf{dpq}^{0/-}$)	−0.42 ($dpp^{0/-}$)	−0.59 ($dpp^{0/-}$)
$[\{(bpy)_2\mathbf{Ru}(dpp)\}_2Ru(\mathbf{dpp})PtCl_2]^{6+}$[c]	1.58 ($2\mathbf{Ru}^{II/III}$)	−0.40 ($\mathbf{dpp}^{0/-}$)	−0.60 ($dpp^{0/-}$)	−0.71 ($dpp^{0/-}$)
$[\{(bpy)_2\mathbf{Ru}(dpp)\}_2Ru(\mathbf{dpq})PtCl_2]^{6+}$	1.59 ($2\mathbf{Ru}^{II/III}$)	−0.08 ($\mathbf{dpq}^{0/-}$)	−0.45 ($dpp^{0/-}$)	−0.62 ($dpp^{0/-}$)
$[\{(bpy)_2\mathbf{Ru}(dpp)\}_2Ru(\mathbf{bpm})PtCl_2]^{6+}$	1.60 ($2\mathbf{Ru}^{II/III}$)	−0.15 ($\mathbf{bpm}^{0/-}$)	−0.56 ($dpp^{0/-}$)	−0.69 ($dpp^{0/-}$)
$[\{(bpy)_2\mathbf{Os}(dpp)\}_2Ru(\mathbf{bpm})PtCl_2]^{6+}$	1.18 ($2\mathbf{Os}^{II/III}$)	−0.16 ($\mathbf{bpm}^{0/-}$)	−0.57 ($dpp^{0/-}$)	−0.68 ($dpp^{0/-}$)
$[\{(bpy)_2\mathbf{Os}(dpp)\}_2Ru(\mathbf{dpq})PtCl_2]^{6+}$	1.10 ($2\mathbf{Os}^{II/III}$)	−0.08 ($\mathbf{dpq}^{0/-}$)	−0.52 ($dpp^{0/-}$)	−0.65 ($dpp^{0/-}$)

[a] Measurements made in deoxygenated CH_3CN at RT with 0.1 M Bu_4NPF_6 electrolyte. Complexes were in PF_6^- salts. bpy = 2,2′-bipyridine, phen = 1,10-phenanthroline, dpp = 2,3-bis(2-pyridyl)pyrazine, dpq = 2,3-bis(2-pyridyl)quinoxaline, bpm = 2,2′-bipyrimidine. [b] From ref 29. [c] From ref 19. [d] From ref 34.

with a diode array with 1 nm resolution and a spectral range of 190 to 1100 nm at RT in spectral grade acetonitrile and a 1 cm path length quartz cuvette. Extinction coefficient experiments were performed in triplicate.

Emission Spectroscopy and Time-Resolved Emission Spectroscopy. Steady state emission spectra were acquired on a QuantaMaster Model QM-200-45E fluorimeter from Photon Technologies, Inc. (PTI). The spectra were corrected for PMT response. Emission quantum yields were measured relative to $[Os(bpy)_3](PF_6)_2$, Φ^{em} = 0.0050 in deoxygenated acetonitrile at RT.[37] Excited state emission lifetime measurements were performed with a PTI PL2300 nitrogen laser pumping a PTI PL 201 continuously tunable dye laser as an excitation source (360−900 nm), and the signal was displayed on a LeCroy 9361 Dual 300 MHz oscilloscope (2.5 Gs/s). RT measurements were performed in deoxygenated spectral grade acetonitrile, and 77 K measurements were performed in a 4:1 (v/v) EtOH/MeOH glass for all experiments.

RESULTS AND DISCUSSION

Synthesis. The tetrametallic complexes were synthesized in high purity using a building block process with control of reaction stoichiometry and reaction conditions, Figure 3. The light absorbing metal M was coordinated to the TLs, followed by incorporation of the dpp ligands. Two $[(TL)_2M(dpp)]^{2+}$ LA units were coupled to a central Ru with addition of the BL following complexation of the *cis*-$PtCl_2$ unit which occurs in the final step because of the reactivity of this complex as a result of RM incorporation. Characterization of the complexes was complicated by isomerization at each Ru and Os center making ^1H NMR spectroscopy not valuable. The complexes were characterized by ESI-MS, electrochemistry, electronic absorption spectroscopy, and emission spectroscopy. Previous reports indicate that a mixture of isomers has a negligible effect on the spectroscopic properties of Ru polyazine bridged supramolecular complexes.[38] Careful purification of the Ru and Os complexes along the synthetic pathway provide for high purity tetrametallics. The coupling of terminal LA units to a remote Pt RM provides for LA units which are electronically less coupled to the Pt RM which should provide enhanced ^{3}MLCT lifetimes for these LA units.

Electrochemistry. The electrochemistry of the complexes gives insight into the orbital energetics in this structural motif, with reversible Ru or Os oxidations and ligand-based reductions with potentials indicative of each subunit identity. All synthons are redox active providing for detection of impurities via careful electrochemical analysis. The trimetallic and tetrametallic complexes exhibit terminal metal-based oxidation processes and ligand-based reduction processes, with μ-$BL^{0/-}$ reductions occurring prior to terminal $BL^{0/-}$ and $TL^{0/-}$ reductions typical of bpm, dpp, and dpq bridged complexes.[3] The central metal-based oxidations occur outside the solvent window, typical of a $Ru(\mu\text{-}BL)_3$ coordination.[39] The reduction potential of a BL is sensitive to its coordination environment, providing a handle for understanding the complicated redox processes. The building block process is critical in evaluation of the redox processes in these complexes; varying a single component between two complexes causes a change in the electrochemistry that can be attributed to that component. The redox properties of the $[\{(TL)_2M(dpp)\}_2Ru(BL)]^{6+}$ and $[\{(TL)_2M(dpp)\}_2Ru(BL)PtCl_2]^{6+}$ complexes are summarized in Table 1. Several $dpp^{-/2-}$, $BL^{-/2-}$ and $TL^{0/-}$ reductions overlap at potentials negative of about −1 V. The electrochemistry of each trimetallic $[\{(TL)_2M(dpp)\}_2Ru(BL)]^{6+}$ complex shows two overlapping $M^{II/III}$ oxidation processes, 1.56−1.61 V (M = Ru) and 1.07−1.16 V (M = Os), due to the largely electronically isolated terminal metal centers. The two dpp ligands undergo two successive reductions in the range −0.42 to −0.71 V, consistent with both dpp ligands being bridging between two electropositive metals and the

dx.doi.org/10.1021/ic200793f |Inorg. Chem. 2011, 50, 8850–8860

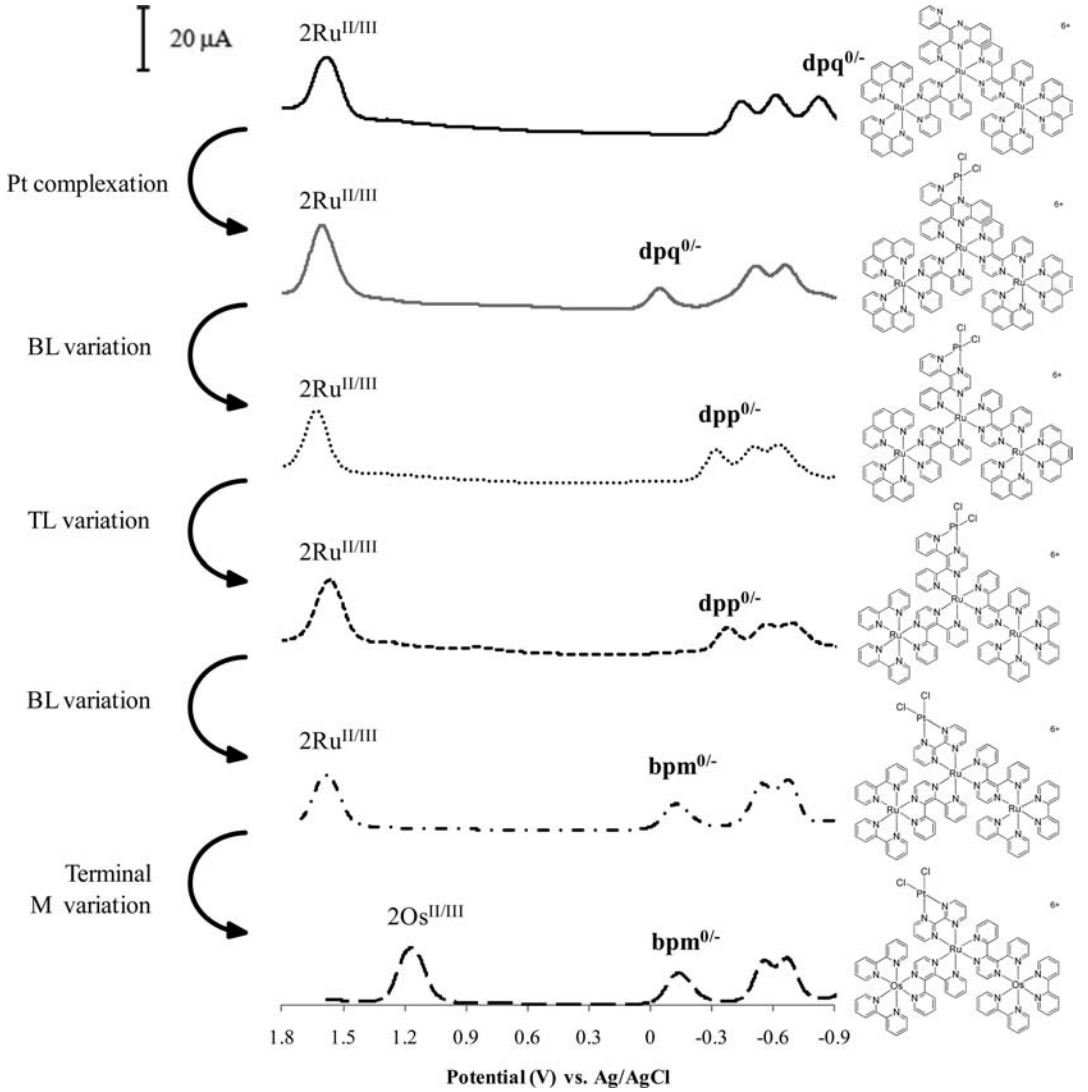

Figure 4. Square wave voltammograms of $[\{(phen)_2Ru(dpp)\}_2Ru(dpq)]^{6+}$ (bold black solid lines), $[\{(phen)_2Ru(dpp)\}_2Ru(dpq)PtCl_2]^{6+}$ (gray solid lines), $[\{(phen)_2Ru(dpp)\}_2Ru(dpp)PtCl_2]^{6+}$ (black dotted lines), $[\{(bpy)_2Ru(dpp)\}_2Ru(dpp)PtCl_2]^{6+}$ (black dashed lines), $[\{(bpy)_2Ru(dpp)\}_2Ru(bpm)PtCl_2]^{6+}$(black dashed-dotted lines), and $[\{(bpy)_2Os(dpp)\}_2Ru(bpm)PtCl_2]^{6+}$ (black bold dashed lines) recorded in 0.1 M Bu_4NPF_6 solution in CH_3CN at RT with potential referenced to Ag/AgCl. bpy = 2,2′-bipyridine, phen = 1,10-phenanthroline, dpp = 2,3-bis(2-pyridyl)pyrazine, dpq = 2,3-bis(2-pyridyl)quinoxaline, bpm = 2,2′-bipyrimidine.

electronic coupling of the two dpp ligands in this motif. The $BL^{0/-}$ couple and the dpp reduction potentials are dictated by the nature of the BL. Reduction of dpq occurs in the range of −0.80 to −0.88 V, while dpp and bpm reduce at similar potentials ranging from −1.00 and −1.08 V. Coordination of the *cis*-$PtCl_2$ unit to the bridging ligand stabilizes the BL π^* orbitals which leads to orbital inversion with the $BL^{0/-}$ couple occurring prior to $dpp^{0/-}$ couples. This is evidenced by a dramatic shift of the $BL^{0/-}$ reduction potential, with the couple at −0.32 to −0.40 V (BL = dpp), −0.05 to −0.08 V (BL = dpq), and −0.15 to −0.16 V (BL = bpm), independent of TL and LA metal. Coordination of a Ru^{II} and Pt^{II} is known to dramatically stabilize $BL^{0/-}$ couples even more than coordination of two Ru^{II} centers.[27]

Figure 4 shows the square wave voltammograms of a series of these complexes illustrating how subunit variation modulates redox properties. Square wave voltammograms for $[\{(phen)_2Ru(dpp)\}_2Ru(dpq)]^{6+}$ and $[\{(phen)_2Ru(dpp)\}_2Ru(dpq)PtCl_2]^{6+}$ show that addition of the *cis*-$PtCl_2$ moiety dramatically impacts the $dpq^{0/-}$ couple with little impact on other subunit redox potentials.

Variation of the BL in the tetrametallic architecture modulates redox properties. The most prominent difference in the electrochemistry of $[\{(bpy)_2Ru(dpp)\}_2Ru(BL)PtCl_2]^{6+}$ (BL = dpp, bpm, and dpq) arises from the varying reduction potentials of the $BL^{0/-}$ couple, dpp (−0.40 V), bpm (−0.15 V), dpq (−0.08 V), consistent with the lower lying π^* acceptor orbitals of dpq versus bpm versus dpp. The oxidation potential of the terminal Ru centers remains largely unaffected (1.58−1.60 V) by BL variation. The two $dpp^{0/-}$ couples also occur at similar potentials (within 150 mV) upon BL modulation. Small changes in the $dpp^{0/-}$ couples result from the BL variation modulated electron density at the central Ru which changes π-backbonding to the dpp ligands. Similar trends are observed for the complexes of the form $[\{(phen)_2Ru(dpp)\}_2Ru(BL)PtCl_2]^{6+}$ (BL = dpp and dpq) and $[\{(bpy)_2Os(dpp)\}_2Ru(BL)PtCl_2]^{6+}$ (BL = bpm and dpq), Table 1. Variation of BL provides a means

dx.doi.org/10.1021/ic200793f |*Inorg. Chem.* 2011, 50, 8850–8860

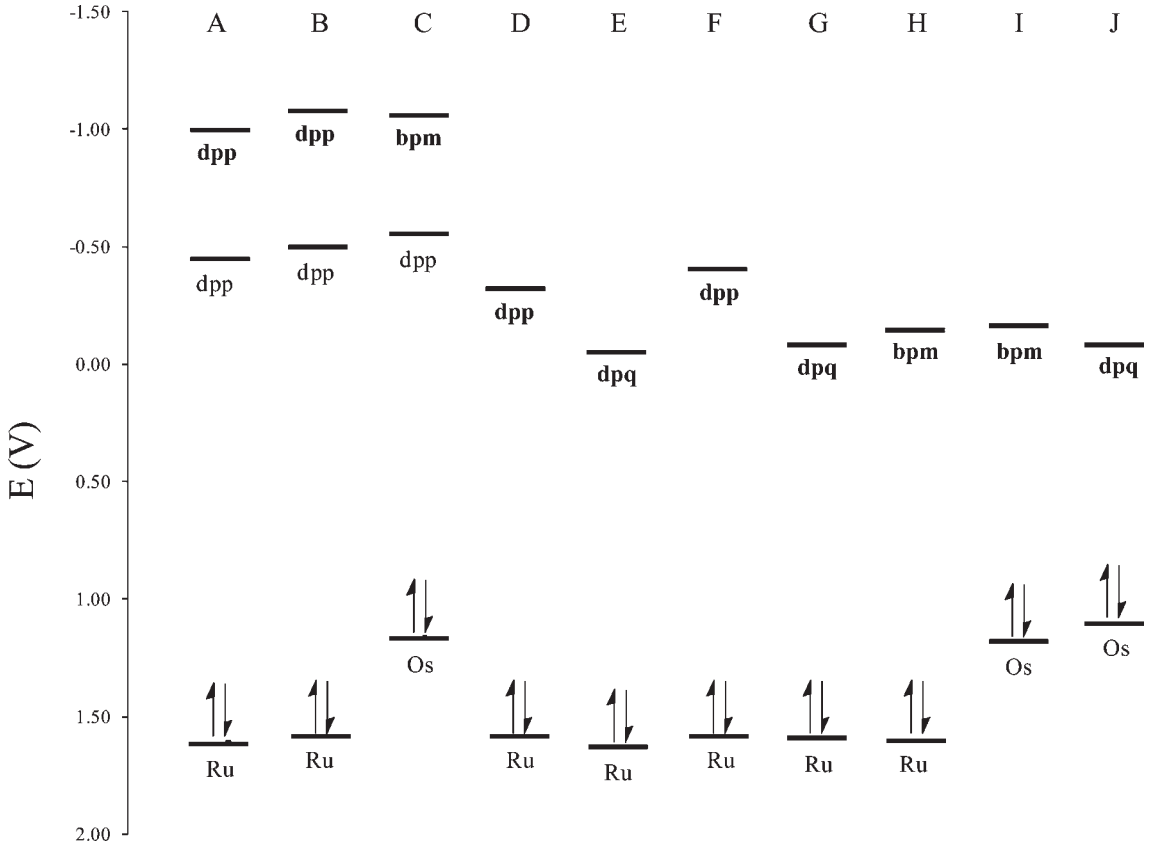

Figure 5. Frontier orbital energetics of (A) $[\{(phen)_2Ru(dpp)\}_2Ru(\mathbf{dpp})]^{6+}$, (B) $[\{(bpy)_2Ru(dpp)\}_2Ru(\mathbf{dpp})]^{6+}$, (C) $[\{(bpy)_2Os(dpp)\}_2Ru(\mathbf{bpm})]^{6+}$, (D) $[\{(phen)_2Ru(dpp)\}_2Ru(\mathbf{dpp})PtCl_2]^{6+}$, (E) $[\{(phen)_2Ru(dpp)\}_2Ru(\mathbf{dpq})PtCl_2]^{6+}$, (F) $[\{(bpy)_2Ru(dpp)\}_2Ru(\mathbf{dpp})PtCl_2]^{6+}$, (G) $[\{(bpy)_2Ru(dpp)\}_2Ru(\mathbf{dpq})PtCl_2]^{6+}$, (H) $[\{(bpy)_2Ru(dpp)\}_2Ru(\mathbf{bpm})PtCl_2]^{6+}$, (I) $[\{(bpy)_2Os(dpp)\}_2Ru(\mathbf{bpm})PtCl_2]^{6+}$, and (J) $[\{(bpy)_2Os(dpp)\}_2Ru(\mathbf{dpq})PtCl_2]^{6+}$ showing orbital inversion upon platination of the trimetallic complexes, simplified by displaying single orbitals from orbital sets with E in volts versus Ag/AgCl. Bold indicates BL between Ru and Pt. bpy = 2,2′-bipyridine, phen = 1,10-phenanthroline, dpp = 2,3-bis(2-pyridyl)pyrazine, dpq = 2,3-bis(2-pyridyl)quinoxaline, bpm = 2,2′-bipyrimidine.

of tuning the energy of the LUMO in this supramolecular architecture.

Varying the LA metal from Ru to Os provides another means of tuning the photochemical and photophysical properties since the HOMO is terminal LA metal based. Tris-chelated polyazine Os^{II} complexes generally oxidize at lower potentials than analogous Ru^{II} complexes.[32] In the tetrametallic complexes $[\{(bpy)_2Ru(dpp)\}_2Ru(bpm)PtCl_2]^{6+}$ and $[\{(bpy)_2Os(dpp)\}_2Ru(bpm)PtCl_2]^{6+}$, the terminal $M^{II/III}$ oxidations occur at 1.60 V (M = Ru) and 1.18 V (M = Os). The $bpm^{0/-}$ and $dpp^{0/-}$ reductions occur at similar potentials regardless of the terminal metal used. The same trend is observed in the electrochemistry of $[\{(bpy)_2Ru(dpp)\}_2Ru(dpq)PtCl_2]^{6+}$ and $[\{(bpy)_2Os(dpp)\}_2Ru(dpq)PtCl_2]^{6+}$, as well as the four trimetallic precursors, Table 1. TL variation from bpy to phen results in small shifts in the terminal Ru couples in the harder to oxidize phen based systems.

Figure 5 illustrates the frontier orbital energetics for selected trimetallics and the series of tetrametallic complexes. The complexes display terminal M based HOMOs and dpp (trimetallic) or BL (tetrametallic) based LUMOs. The LUMO energy is lowest when BL = dpq and highest when BL = dpp, and the HOMO is destabilized when M = Os in comparison to Ru. The tetrametallic complexes exhibit spatial separation between the HOMO localized on the terminal metal and the LUMO localized on the bridging ligand between central Ru and Pt. This localization of the HOMO and LUMO with resultant spatial separation suggests a lowest-lying charge separated state (CS), with an oxidized terminal Ru or Os and a reduced BL, with analogous trimetallics displaying the same emissive M→dpp ^{3}MLCT state but lacking a CS state.

Electronic Absorption Spectroscopy. The trimetallic and tetrametallic complexes are efficient light absorbers, with overlapping contributions from ligand $\pi\rightarrow\pi^*$ transitions dominating the UV region and MLCT transitions dominating the visible region. The electronic absorption transitions and assignments for the trimetallics and tetrametallics are summarized in Table 2. Addition of a *cis*-$PtCl_2$ unit does not greatly affect the charge transfer transitions of the tetrametallic complexes relative to their trimetallic synthons, indicating that a reactive metal can be covalently bound to a large chromophore while maintaining its light absorbing properties, shown for $[\{(bpy)_2Ru(dpp)\}_2Ru(dpq)]^{6+}$ and $[\{(bpy)_2Ru(dpp)\}_2Ru(dpq)PtCl_2]^{6+}$ in Figure 6A. The electronic absorption spectra for $[\{(bpy)_2Ru(dpp)\}_2Ru(bpm)PtCl_2]^{6+}$ and $[\{(bpy)_2Os(dpp)\}_2Ru(bpm)PtCl_2]^{6+}$ are presented in Figure 6B, illustrating the impact of terminal metal variation. The complexes with TL = bpy have bpy $\pi\rightarrow\pi^*$ transitions about 290 nm and those with TL = phen display phen $\pi\rightarrow\pi^*$ transitions at 262 nm, independent of BL. Each complex contains μ-dpp ligands between the light absorbing metals as well as broad, lowest-lying $Ru(d\pi)\rightarrow dpp(\pi^*)$ ^{1}MLCT transitions when M = Ru occurring at about 540 nm. These broad transitions also receive contribution from underlying $Ru(d\pi)\rightarrow BL(\pi^*)$ CT

dx.doi.org/10.1021/ic200793f |*Inorg. Chem.* 2011, 50, 8850–8860

Table 2. Electronic Absorption Spectroscopy Data for $[\{(TL)_2M(dpp)\}_2Ru(BL)]^{6+}$ and $[\{(TL)_2M(dpp)\}_2Ru(BL)PtCl_2]^{6+}$.[a]

complex	λ_{max}^{abs} (nm)	$\varepsilon \times 10^{-4}$ (M^{-1} cm^{-1})	assignment
		Trimetallics	
$[\{(phen)_2Ru(dpp)\}_2Ru(dpp)]^{6+}$	262	16.6	phen $\pi\rightarrow\pi^*$
	340	4.2	dpp $\pi\rightarrow\pi^*$
	421	2.8	Ru(dπ)$\rightarrow$phen(π^*) CT
	543	3.4	Ru(dπ)$\rightarrow$dpp(π^*) CT
$[\{(phen)_2Ru(dpp)\}_2Ru(dpq)]^{6+b}$	262	15.9	phen $\pi\rightarrow\pi^*$
	350 (sh)	4.8	dpp $\pi\rightarrow\pi^*$, dpq $\pi\rightarrow\pi^*$
	415	2.6	Ru(dπ)$\rightarrow$phen(π^*) CT
	541	3.8	Ru(dπ)$\rightarrow$dpp(π^*) CT, Ru(dπ)$\rightarrow$dpq(π^*) CT
$[\{(bpy)_2Ru(dpp)\}_2Ru(dpp)]^{6+c}$	290	12.2	bpy $\pi\rightarrow\pi^*$
	340 (sh)	4.8	dpp $\pi\rightarrow\pi^*$
	416	2.4	Ru(dπ)$\rightarrow$bpy(π^*) CT
	542	3.6	Ru(dπ)$\rightarrow$dpp(π^*) CT
$[\{(bpy)_2Ru(dpp)\}_2Ru(dpq)]^{6+d}$	292	12.5	bpy $\pi\rightarrow\pi^*$
	330 (sh)	5.5	dpp $\pi\rightarrow\pi^*$, dpq $\pi\rightarrow\pi^*$
	420	2.0	Ru(dπ)$\rightarrow$bpy(π^*) CT
	540	4.0	Ru(dπ)$\rightarrow$dpp(π^*) CT, Ru(dπ)$\rightarrow$dpq(π^*) CT
$[\{(bpy)_2Ru(dpp)\}_2Ru(bpm)]^{6+}$	286	10.4	bpy $\pi\rightarrow\pi^*$
	320	4.8	dpp $\pi\rightarrow\pi^*$, bpm $\pi\rightarrow\pi^*$
	423	2.1	Ru(dπ)$\rightarrow$bpy(π^*) CT
	542	3.4	Ru(dπ)$\rightarrow$dpp(π^*) CT
$[\{(bpy)_2Os(dpp)\}_2Ru(bpm)]^{6+}$	282	9.6	bpy $\pi\rightarrow\pi^*$
	350	4.1	dpp $\pi\rightarrow\pi^*$, bpm $\pi\rightarrow\pi^*$
	425	2.2	Os(dπ)$\rightarrow$bpy(π^*) CT
	560	3.7	Os(dπ)$\rightarrow$dpp (π^*) CT, Ru(dπ)$\rightarrow$dpp(π^*) CT, Ru(dπ)$\rightarrow$bpm(π^*) CT
	720	1.0	Os(dπ)$\rightarrow$dpp (π^*) ^{3}MLCT
$[\{(bpy)_2Os(dpp)\}_2Ru(dpq)]^{6+d}$	282	11.0	bpy $\pi\rightarrow\pi^*$
	340 (sh)	5.0	dpq $\pi\rightarrow\pi^*$, dpp $\pi\rightarrow\pi^*$
	430	1.8	Os(dπ)$\rightarrow$bpy(π^*) CT
	560	3.3	Os(dπ)$\rightarrow$dpp (π^*) CT, Ru(dπ)$\rightarrow$dpp(π^*) CT
	720	0.9	Os(dπ)$\rightarrow$dpp (π^*) ^{3}MLCT
		Tetrametallics	
$[\{(phen)_2Ru(dpp)\}_2Ru(dpp)PtCl_2]^{6+}$	262	15.5	phen $\pi\rightarrow\pi^*$
	330 (sh)	5.6	dpp $\pi\rightarrow\pi^*$
	421	2.9	Ru(dπ)$\rightarrow$phen(π^*) CT
	543	4.2	Ru(dπ)$\rightarrow$dpp(π^*) CT
$[\{(phen)_2Ru(dpp)\}_2Ru(dpq)PtCl_2]^{6+b}$	262	15.0	phen $\pi\rightarrow\pi^*$
	350 (sh)	4.8	dpp $\pi\rightarrow\pi^*$, dpq $\pi\rightarrow\pi^*$
	415	3.2	Ru(dπ)$\rightarrow$phen(π^*) CT
	541	3.8	Ru(dπ)$\rightarrow$dpp(π^*) CT, Ru(dπ)$\rightarrow$dpq(π^*) CT
$[\{(bpy)_2Ru(dpp)\}_2Ru(dpp)PtCl_2]^{6+c}$	290	10.0	bpy $\pi\rightarrow\pi^*$
	320 (sh)	5.5	dpp $\pi\rightarrow\pi^*$
	416	2.2	Ru(dπ)$\rightarrow$bpy(π^*) CT
	542	3.5	Ru(dπ)$\rightarrow$dpp(π^*) CT
$[\{(bpy)_2Ru(dpp)\}_2Ru(dpq)PtCl_2]^{6+}$	290	9.0	bpy $\pi\rightarrow\pi^*$
	320 (sh)	4.6	dpp $\pi\rightarrow\pi^*$
	360 (sh)	4.2	dpq $\pi\rightarrow\pi^*$
	416	2.0	Ru(dπ)$\rightarrow$bpy(π^*) CT
	542	3.3	Ru(dπ)$\rightarrow$dpp(π^*) CT, Ru(dπ)$\rightarrow$dpq(π^*) CT
$[\{(bpy)_2Ru(dpp)\}_2Ru(bpm)PtCl_2]^{6+}$	286	10.2	bpy $\pi\rightarrow\pi^*$
	320 (sh)	5.1	dpp $\pi\rightarrow\pi^*$, bpm $\pi\rightarrow\pi^*$
	422	2.3	Ru(dπ)$\rightarrow$bpy(π^*) CT
	542	3.3	Ru(dπ)$\rightarrow$dpp(π^*) CT, Ru(dπ)$\rightarrow$bpm(π^*) CT

dx.doi.org/10.1021/ic200793f |*Inorg. Chem.* 2011, 50, 8850–8860

Table 2. Continued

complex	λ_{max}^{abs} (nm)	$\varepsilon \times 10^{-4}$ (M^{-1} cm^{-1})	assignment
$[\{(bpy)_2Os(dpp)\}_2Ru(bpm)PtCl_2]^{6+}$	282	9.5	bpy $\pi \rightarrow \pi^*$
	350 (sh)	4.6	dpp $\pi \rightarrow \pi^*$, bpm $\pi \rightarrow \pi^*$
	420	2.7	$Os(d\pi) \rightarrow bpy(\pi^*)$ CT
	560	3.8	$Os(d\pi) \rightarrow dpp\ (\pi^*)$ CT, $Ru(d\pi) \rightarrow dpp(\pi^*)$ CT, $Ru(d\pi) \rightarrow bpm(\pi^*)$ CT
	720	1.2	$Os(d\pi) \rightarrow dpp\ (\pi^*)$ ^{3}MLCT
$[\{(bpy)_2Os(dpp)\}_2Ru(dpq)PtCl_2]^{6+}$	282	10.5	bpy $\pi \rightarrow \pi^*$
	320 (sh)	5.2	dpp $\pi \rightarrow \pi^*$
	360 (sh)	4.2	dpq $\pi \rightarrow \pi^*$
	420	2.7	$Os(d\pi) \rightarrow bpy(\pi^*)$ CT
	540	3.3	$Ru(d\pi) \rightarrow dpp(\pi^*)$ CT
	556	3.5	$Os(d\pi) \rightarrow dpp\ (\pi^*)$ CT
	650−800	1.5	$Os(d\pi) \rightarrow dpp\ (\pi^*)$ ^{3}MLCT

[a] Measurements made in deoxygenated CH_3CN at RT with complexes as PF_6^- salts. bpy = 2,2′-bipyridine, phen = 1,10-phenanthroline, dpp = 2,3-bis-(2-pyridyl)pyrazine, dpq = 2,3-bis(2-pyridyl)quinoxaline, bpm = 2,2′-bipyrimidine. [b] From ref 29. [c] From ref 19. [d] From ref 34.

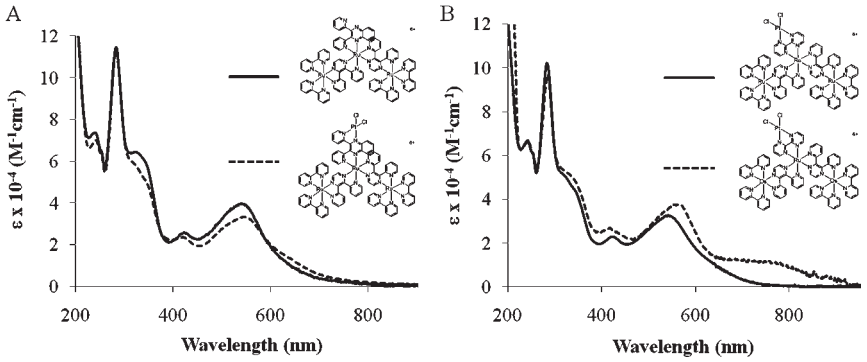

Figure 6. Electronic absorption spectra of (a) $[\{(bpy)_2Ru(dpp)\}_2Ru(dpq)]^{6+}$ (black solid lines) and $[\{(bpy)_2Ru(dpp)\}_2Ru(dpq)PtCl_2]^{6+}$ (black dashed lines) and (b) $[\{(bpy)_2Ru(dpp)\}_2Ru(bpm)PtCl_2]^{6+}$ (black solid lines) and $[\{(bpy)_2Os(dpp)\}_2Ru(bpm)PtCl_2]^{6+}$ (black dashed lines) in CH_3CN solution. bpy = 2,2′-bipyridine, dpp = 2,3-bis(2-pyridyl)pyrazine, dpq = 2,3-bis(2-pyridyl)quinoxaline, bpm = 2,2′-bipyrimidine.

transitions, providing small differences in molar absorptivity and band shape. When M = Os, the lowest-lying ^{1}MLCT transition red shifts to about 560 nm, as the $Os(d\pi) \rightarrow dpp(\pi^*)$ CT transitions are red-shifted. The Os complexes also extend their light absorbing properties to the 650−800 nm region with ^{3}MLCT transitions gaining intensity from significant spin−orbit coupling.

Emission Spectroscopy and Photophysics. Ru-polyazine complexes emit from their ^{3}MLCT excited states, providing a probe into their excited state dynamics and reactivity. Typically upon optical excitation to populate ^{1}MLCT excited states, intersystem crossing occurs with unit efficiency to populate the emissive ^{3}MLCT state.[1] Steady state and time-resolved emission spectroscopy data for each complex in acetonitrile at RT and at 77 K in a 4:1 EtOH/MeOH rigid matrix are summarized in Table 3. This structural motif provides for a unique forum to explore the role and excited state dynamics of the CS state as all the M = Ru trimetallic and tetrametallic systems display a lowest lying emissive terminal $Ru \rightarrow dpp$ ^{3}MLCT state similar in nature and energy throughout the series of complexes.

The Os complexes have lower energy ^{1}MLCT excited states and do not display detectable emission. The Ru based trimetallic and tetrametallic complexes emit from the low-lying terminal $Ru(d\pi) \rightarrow dpp(\pi^*)$ ^{3}MLCT state; however, the tetrametallic complexes display dramatically quenched quantum yields for emission (Φ^{em}) and shortened excited state lifetimes (τ) at RT relative to their trimetallic synthons. This is indicative of intramolecular electron transfer to populate the nonemissive ^{3}CS state, formally terminal $Ru(d\pi) \rightarrow BL(\pi^*)$. Further support of quenching via electron transfer comes from the similar excited state lifetime in rigid glass at 77 K for each tetrametallic and its trimetallic synthon. Electron transfer is impeded in rigid media at low temperatures. Interestingly, quantitative analysis of the degree of quenching of the emission versus the reduction in excited state lifetime suggests the emissive state in the tetrametallic motif is not populated with unit efficiency. Equations 1 and 2 relate the excited state lifetimes to rate constants that deactivate the emissive ^{3}MLCT excited state,

$$\tau_{model} = \frac{1}{k_r + k_{nr}} \quad (1)$$

$$\tau_{tetrametallic} = \frac{1}{k_r + k_{nr} + k_{et}} \quad (2)$$

where k_r is the rate constant for radiative decay, k_{nr} is the rate constant for nonradiate decay, and k_{et} is the rate constant for intramolecular electron transfer. The rate constants for k_r and k_{nr} of the tetrametallic are assumed to be equal to those of the trimetallic model because of the similar nature and energy of the emissive state. The k_{et} for the dpq versus dpp complexes

dx.doi.org/10.1021/ic200793f |Inorg. Chem. 2011, 50, 8850–8860

Table 3. Photophysical Data at RT and 77 K[a]

complex	RT						77 K	
	λ^{em} (nm)	$\Phi^{em} \times 10^3$	τ (μs)	$k_r \times 10^{-3}$ (s^{-1})[b]	$k_{nr} \times 10^{-6}$ (s^{-1})[b]	$k_{et} \times 10^{-6}$ (s^{-1})	λ^{em} (nm)	τ (μs)
Trimetallics								
$[\{(phen)_2Ru(dpp)\}_2Ru(dpp)]^{6+}$	760	1.01	0.11	9.2	9.1		705	2.1
$[\{(phen)_2Ru(dpp)\}_2Ru(dpq)]^{6+}$[c]	752	1.01	0.11	9.2	9.1		715	1.7
$[\{(bpy)_2Ru(dpp)\}_2Ru(dpp)]^{6+}$[d]	747	0.61	0.13	4.7	7.7		698	1.7
$[\{(bpy)_2Ru(dpp)\}_2Ru(dpq)]^{6+}$[e]	745	0.60	0.13	4.6	7.7		710	1.7
$[\{(bpy)_2Ru(dpp)\}_2Ru(bpm)]^{6+}$	753	0.49	0.13	3.8	7.7		700	1.7
Tetrametallics								
$[\{(phen)_2Ru(dpp)\}_2Ru(dpp)PtCl_2]^{6+}$	756	0.71	0.083	9.2	9.1	3.0	705	2.1
$[\{(phen)_2Ru(dpp)\}_2Ru(dpq)PtCl_2]^{6+}$[c]	752	0.32	0.080	9.2	9.1	3.4	715	1.7
$[\{(bpy)_2Ru(dpp)\}_2Ru(dpp)PtCl_2]^{6+}$[d]	750	0.32	0.10	4.7	7.7	2.3	712	1.7
$[\{(bpy)_2Ru(dpp)\}_2Ru(dpq)PtCl_2]^{6+}$	745	0.25	0.092	4.6	7.7	3.2	703	1.7
$[\{(bpy)_2Ru(dpp)\}_2Ru(bpm)PtCl_2]^{6+}$	753	0.06	0.10	3.8	7.7	2.3	700	1.7

[a] RT measurements were performed on CH_3CN solutions of PF_6^- salts deoxygenated by bubbling with Ar. 77 K measurements were performed in a 4:1 EtOH/MeOH glass. Values corrected for PMT response. [b] Values for the tetrametallic complexes are assumed to be the same as the values for the corresponding trimetallic complexes. [c] From ref 29. [d] From ref 19. [e] From ref 34.

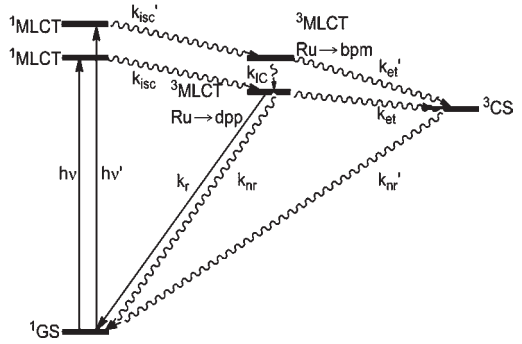

Figure 7. State diagram for $[\{(bpy)_2Ru(dpp)\}_2Ru(bpm)PtCl_2]^{6+}$ (bpy = 2,2′-bipyridine, dpp = 2,3-bis(2-pyridyl)pyrazine, bpm = 2,2′-bipyrimidine). GS = ground state, k_{isc} = rate constant for intersystem crossing, k_{IC} = rate constant for internal conversion, k_r = rate constant for radiative decay, k_{nr} = rate constant for nonradiative decay, k_{et} = rate constant for electron transfer.

increases with increased driving force for intramolecular electron transfer to populate the CS state as expected. Intramolecular electron transfer can also be probed through Φ^{em} in eqs 3 and 4.

$$\Phi^{em(model)}_{^3MLCT} = \Phi^{pop(model)}_{^3MLCT}\left(\frac{k_r}{k_r + k_{nr}}\right) \quad (3)$$

$$\Phi^{em(tetrametallic)}_{^3MLCT} = \Phi^{pop(tetrametallic)}_{^3MLCT}\left(\frac{k_r}{k_r + k_{nr} + k_{et}}\right) \quad (4)$$

Unlike typical Ru polyazine complexes, Φ^{pop} of the emissive ^{3}MLCT cannot be unity for the tetrametallic complexes. In all cases the Φ^{em} is quenched more dramatically than suggested by k_{et} calculated by the above lifetime analysis. The reduction in Φ^{em} is larger than the reduction of τ, suggesting a secondary intramolecular electron transfer pathway, k_{et}', responsible for direct population of the ^{3}CS state without passage through the emissive state; however, other pathways may be possible. This data is consistent throughout this series of complexes and in multiple samples on each complex. In all cases a central Ru→BL CT state lies above the emissive Ru→dpp ^{3}MLCT state, and it is feasible for direct population of the CS state via intramolecular electron transfer from the terminal Ru to the central Ru. A state diagram for $[\{(bpy)_2Ru(dpp)\}_2Ru(bpm)PtCl_2]^{6+}$ is depicted in Figure 7.

Equation 4 was used to determine the quantum yields of population of the emissive ^{3}MLCT excited state for the tetrametallic complexes. Upon excitation, the emissive state of $[\{(phen)_2Ru(dpp)\}_2Ru(dpp)PtCl_2]^{6+}$ is populated with Φ = 0.93, indicating a small degree of coupling of the higher-lying ^{3}MLCT state with the ^{3}CS state. Population of the emissive state in $[\{(bpy)_2Ru(dpp)\}_2Ru(dpp)PtCl_2]^{6+}$ is lower with Φ = 0.68, providing a higher level of population of the CS state via a higher lying state. The emissive ^{3}MLCT state of $[\{(bpy)_2Ru(dpp)\}_2Ru(bpm)PtCl_2]^{6+}$ is populated with Φ = 0.16 which indicates a large degree of population of the nonemissive ^{3}CS state via a higher lying state with enhanced k_{et}'. Quantum yields of population of the emissive state are lower when BL = dpq than each BL = dpp analogue for both bpy and phen complexes (Φ = 0.44 and 0.59 for $[\{(phen)_2Ru(dpp)\}_2Ru(dpq)PtCl_2]^{6+}$ and $[\{(bpy)_2Ru(dpp)\}_2Ru(dpq)PtCl_2]^{6+}$, respectively). This suggests the higher lying Ru→BL ^{3}MLCT state directly populates the low-lying ^{3}CS state when BL = dpq or bpm. These states are expected to be lower energy because of the more stabilized BL π^* orbitals.

CONCLUSIONS

A series of eight new structurally diverse complexes of the motifs $[\{(TL)_2M(dpp)\}_2Ru(BL)]^{6+}$ and $[\{(TL)_2M(dpp)\}_2Ru(BL)PtCl_2]^{6+}$, where TL = bpy and phen, BL = dpp, dpq, or bpm, and M = Ru or Os, were synthesized in a building block method. The redox, spectroscopic, and photophysical properties were investigated. Variation of TL, BL, and M as well as comparison between trimetallic and analogous tetrametallic provide for better understanding of the complicated redox processes and excited state dynamics in this motif. This supramolecular architecture provides for terminal Ru or Os based HOMOs and dpp based trimetallic LUMOs and BL based tetrametallic LUMOs which result from BL(π^*) orbital stabilization when complexed

dx.doi.org/10.1021/ic200793f |Inorg. Chem. 2011, 50, 8850–8860

to a Pt(II) moiety. Both the trimetallic and the tetrametallic complexes are efficient UV and visible light absorbers. TL variation from bpy to phen results in higher energy TL $\pi \rightarrow \pi^*$ transitions, and BL variation has little impact on the spectroscopy. The lowest lying ^{1}MLCT transitions are intense because of the number of Ru($d\pi$)→dpp(π^*) CT transitions overlapping in that region. This supramolecular architecture can be manipulated to absorb longer wavelengths by incorporation of Os in the place of terminal Ru. Coordination of Pt does not greatly alter the electronic absorption spectra, allowing the light absorbing properties to be maintained. All these M = Ru complexes display a terminal Ru→μ-dpp ^{3}MLCT emissive excited state that is similar in energy and nature when TL = bpy or phen, BL = dpp, dpq, or bpm and for trimetallic and tetrametallic systems. Intramolecular electron transfer occurs in the tetrametallic complexes from MLCT states to populate a terminal Ru to BL to populate a charge separated state that is spatially separated by the central $(dpp)_2Ru^{II}$ unit. The M = Ru systems populate an emissive Ru($d\pi$)→dpp(π^*) ^{3}MLCT state at RT and 77 K. The emission of all the $[\{(TL)_2Ru(dpp)\}_2Ru(BL)PtCl_2](PF_6)_6$ complexes is quenched at RT but not at 77 K via intramolecular electron transfer to populate the CS state at RT, impeded in rigid matrix at 77 K. The photophysical dynamics of these complexes are unusual, with population of the CS state occurring by at least two pathways and population of the emissive ^{3}MLCT state not occurring with unit efficiency. This is evidenced by dramatically reduced Φ^{em} in the tetrametallics with smaller reductions in the lifetime of the emissive state. Enhanced driving force for intramolecular electron transfer provides for enhanced k_{et} in systems with k_{et} for BL = dpq being larger than BL = dpp. The BL = bpm systems have rather large k_{et}' for indirect population of the CS state. The title complexes provide for terminal LA units with long-lived ^{3}MLCT states remotely coupled to Pt RM sites providing for extended lifetimes to undergo photochemistry. Work is underway to probe the photochemistry of these interesting supramolecular assemblies.

AUTHOR INFORMATION

Corresponding Author
*E-mail: kbrewer@vt.edu.

ACKNOWLEDGMENT

Acknowledgment is made to Travis White, Jing Wang, and Avijita Jain for their contributions to this research, and the Chemical Sciences, Geosciences and Biosciences Division, Office of Basic Energy Sciences, Office of Sciences, U.S. Department of Energy (DE FG02-05ER15751) for their generous support of the development of new LAs used in this research.

REFERENCES

(1) Kalyanasundaram, K. *Coord. Chem. Rev.* **1982**, *46*, 159–244.
(2) Juris, A.; Balzani, V.; Barigelletti, F.; Campagna, S.; Belser, P.; von Zelewsky, A. *Coord. Chem. Rev.* **1988**, *84*, 85–277.
(3) Balzani, V.; Juris, A.; Venturi, M.; Campagna, S.; Serroni, S. *Chem. Rev.* **1996**, *96*, 759–834.
(4) Campagna, S.; Puntoriero, F.; Nastasi, F.; Bergamini, G.; Balzani, V. *Top. Curr. Chem.* **2007**, *280*, 117–214.
(5) Housecroft, C. E.; McCleverty, J. A.; Meyer, T. J. In *Comprehensive. Coordination Chemistry II*; Pergamon: Oxford, U.K., 2003; pp 555−731.
(6) Meyer, T. J. *Pure Appl. Chem.* **1986**, *58*, 1193–1206.
(7) Kumaresan, D.; Shankar, K.; Vaidya, S.; Schmehl, R. H. *Top. Curr. Chem.* **2007**, *281*, 101–142.
(8) Wallace, A. W.; Murphy, W. R., Jr.; Petersen, J. D. *Inorg. Chim. Acta* **1989**, *166*, 47–54.
(9) Braunstein, C. H.; Baker, A. D.; Strekas, T. C.; Gafney, H. D. *Inorg. Chem.* **1984**, *23*, 857–864.
(10) Fuchs, Y.; Lofters, S.; Dieter, T.; Shi, W.; Morgan, R.; Strekas, T. C.; Gafney, H. D.; Baker, A. D. *J. Am. Chem. Soc.* **1987**, *109*, 2691–2697.
(11) Berger, R. M. *Inorg. Chem.* **1990**, *29*, 1920–1924.
(12) Brewer, K. J.; Murphy, W. R., Jr.; Spurlin, S. R.; Petersen, J. D. *Inorg. Chem.* **1986**, *25*, 882–884.
(13) Tinker, L. L.; McDaniel, N. D.; Bernhard, S. *J. Mater. Chem.* **2009**, *19*, 3328–3337.
(14) Wang, M.; Na, Y.; Gorlov, M.; Sun, L. *Dalton Trans.* **2009**, 6458–6467.
(15) Higgins, S. L. H.; White, T. A.; Winkel, B. S. J.; Brewer, K. J. *Inorg. Chem.*, **2011**, *50*, 463−470.
(16) Milkevitch, M.; Brauns, E.; Brewer, K. J. *Inorg. Chem.* **1996**, *35*, 1737–1739.
(17) Swavey, S.; Fang, Z.; Brewer, K. J. *Inorg. Chem.* **2002**, *41*, 2598–2607.
(18) Williams, R. L.; Toft, H. N.; Winkel, B.; Brewer, K. J. *Inorg. Chem.* **2003**, *42*, 4394–4400.
(19) Miao, R.; Mongelli, M. T.; Zigler, D. F.; Winkel, B. S. J.; Brewer, K. J. *Inorg. Chem.* **2006**, *45*, 10413–10415.
(20) Jain, A.; Wang, J.; Mashack, E. R.; Winkel, B. S. J.; Brewer, K. J. *Inorg. Chem.* **2009**, *48*, 9077–9084.
(21) Sahai, R. *Inorg. Chim. Acta* **1986**, *118*, L35.
(22) Yam, V. W.-W.; Lee, V. W.-M.; Cheung, K.-K. *J. Chem. Soc., Chem. Commun.* **1994**, 2075–2076.
(23) Yam, V. W.-W.; Lee, V. W.-M.; Cheung, K.-K. *Organometallics* **1997**, *16*, 2833–2841.
(24) Masaoka, S.; Mukawa, Y.; Sakai, K. *Dalton Trans.* **2010**, *39*, 5868–5876.
(25) Ozawa, H.; Haga, M.; Sakai, K. *J. Am. Chem. Soc.* **2006**, *128*, 4926–4927.
(26) Ozawa, H.; Kobayashi, M.; Balan, B.; Masaoka, S.; Sakai, K. *Chem.—Asian. J.* **2010**, *5*, 1860–1869.
(27) Sahai, R.; Rillema, D. P. *J. Chem. Soc., Chem. Commun.* **1986**, 1133–1134.
(28) Sommovigo, M.; Denti, G.; Serroni, S.; Campagna, S.; Mingazzini, C.; Mariotti, C.; Juris, A. *Inorg. Chem.* **2001**, *40*, 3318–3323.
(29) Knoll, J. D.; Arachchige, S. M.; Brewer, K. J. *ChemSusChem* **2011**, *4*, 252−261.
(30) Sullivan, B. P.; Salmon, D. J.; Meyer, T. J. *Inorg. Chem.* **1978**, *17*, 3334–3341.
(31) Kober, E. M.; Caspar, J. V.; Sullivan, B. P.; Meyer, T. J. *Inorg. Chem.* **1988**, *27*, 4587–4598.
(32) Richter, M. M.; Brewer, K. J. *Inorg. Chim. Acta* **1991**, *180*, 125–131.
(33) Puntoriero, F.; Serroni, S.; Licciardello, A.; Venturi, M.; Juris, A.; Ricevuto, V.; Campagna, S. *J. Chem. Soc., Dalton Trans.* **2001**, 1035–1042.
(34) Brauns, E.; Jones, S. W.; Clark, J. A.; Molnar, S. M.; Kawanishi, Y.; Brewer, K. J. *Inorg. Chem.* **1997**, *36*, 2861–2867.
(35) Price, J. H.; Williamson, A. N.; Schramm, R. F.; Wayland, B. B. *Inorg. Chem.* **1972**, *11*, 1280–1284.
(36) Goodwin, H. A.; Lions, F. *J. Am. Chem. Soc.* **1959**, *81*, 6415–6422.
(37) Caspar, J. V.; Kober, E. M.; Sullivan, B. P.; Meyer, T. J. *J. Am. Chem. Soc.* **1982**, *104*, 630–632.
(38) MacDonnell, F. M.; Bodige, S. *Inorg. Chem.* **1996**, *35*, 5758–5759.
(39) Ceroni, P.; Paolucci, F.; Paradisi, C.; Juris, A.; Roffia, S.; Serroni, S.; Campagna, S.; Bard, A. J. *J. Am. Chem. Soc.* **1998**, *120*, 5480–5487.